

Critical slowing down in the two-dimensional Ising model measured using ferromagnetic ultrathin films

M. J. Dunlavy* and D. Venus

Department of Physics and Astronomy, McMaster University, 1280 Main St. West, Hamilton, Ontario, Canada

(Received 3 September 2004; published 12 April 2005)

Power-law scaling of the relaxation time τ associated with critical slowing down has been experimentally measured in the dynamics of the magnetization of a bilayer of iron grown on top of a $W(110)$ substrate using the complex magnetic ac susceptibility $\chi(T)$. The observed value of the critical exponent for the slowing down above the Curie transition of this two-dimensional Ising ferromagnetic system is $z\nu=2.09\pm 0.06$ (95% confidence), in agreement with most contemporary theories and simulations. Further analysis reveals that dynamical effects cause $\chi(T)$ to deviate from power-law scaling as the temperature is decreased towards T_c , whereas the saturation of the correlation length due to finite-size effects (on the order of 500 lattice spaces) limits the divergence of τ .

DOI: 10.1103/PhysRevB.71.144406

PACS number(s): 75.70.Rf, 75.40.Gb, 75.70.Ak

I. INTRODUCTION

The experimental verification of the critical exponents associated with the dynamic universality classes has proven to be a continuing experimental challenge long after the theoretical groundwork for the field was laid in the 1960s.¹ Although a great deal of experimental and theoretical consensus has emerged for the static critical exponents,² this is not the case for the slowing-down exponent, z , about which important discrepancies remain even in the three-dimensional (3D) classes, which are relatively simple to realize in our three-dimensional world. Some recent examples include the 3D Heisenberg model,^{3,4} the 3D Ising model,⁵ and the 3D XY model as applied to high- T_c superconductors.⁶ Even more problematic are the two-dimensional (2D) Heisenberg model,⁷ where it is difficult to find a system without anisotropy, and the 2D XY model, for which the Kosterlitz-Thouless transition plays a prominent role.⁸ However, it is perhaps surprising that fundamental inconsistencies between the experimental and theoretical determinations of z remain in one of the conceptually simplest classes: the 2D Ising model.

The dynamic behavior of the 2D Ising model has gained prominence in recent years, due to the interest in the fundamental properties and applications of ultrathin ferromagnetic films. It has been known for many years that it is possible to fabricate high-quality ferromagnetic films of only a few atomic layers and form true two-dimensional samples, in contradiction to the Mermin-Wagner theorem.⁹ This occurs due to the presence of magnetic anisotropies which transform the universality class of a ferromagnetic monolayer to the 2D Ising model close to the magnetic phase transition.¹⁰ Experiments have confirmed 2D Ising static critical exponents using various surface magnetometry techniques such as the Kerr effect and spin-polarized spectroscopies.¹¹ A couple of examples are the critical exponent of the magnetization β (Refs. 12–14) and of the susceptibility, γ .¹⁵

There have been many theoretical and computational studies of critical slowing down for the 2D Ising class magnetic system (which belongs to model A in the Hohenberg

and Halperin hierarchy of dynamic universality classes¹). Lacasse *et al.*¹⁶ gave an excellent survey of this work up to 1993, and Nightingale and Blöte¹⁷ listed additional results up to 1996. As simulations and theories became more sophisticated, most current studies placed the value of z between 2.1 and 2.25, with many theoretical results clustered near 2.13. These values of z conform to the prediction from expansions about $D=4$ and other methods that the dynamic critical exponent has a lower bound of 2 in the Ising universality classes.^{18–21}

The experimental investigations of dynamical scaling have been confined to a few studies of layered bulk antiferromagnetic materials which approach the 2D Ising model because of the very small effective exchange between layers. Slivka *et al.* found $z=1.77\pm 0.05$ for $KFeF_4$,²² and Keller and Savic found 1.29 ± 0.09 for the same material,²³ both using Mössbauer spectroscopy. Hutchings *et al.* found 1.69 ± 0.05 for Rb_2CoF_4 ,²⁴ using neutron scattering. All of these results are less than the theoretical minimum value, but the reasons behind this discrepancy are unclear.

Ultrathin ferromagnetic films provide an alternate system for the study of critical slowing down in two dimensions that may have advantages over layered bulk antiferromagnetics. First, the extreme ratio between the film thickness (on the order of atomic layers) and the lateral film length allow for the design and fabrication of true two-dimensional structures, where the critical properties do not vary over the thickness of the film. Second, disturbances in the magnetization near the transition can be created by a small applied field, whereas studies using antiferromagnets must wait for the magnetic excitations to be spontaneously created and stabilized on a time scale that diverges and becomes prohibitive in the important temperature range close to the transition. Finally, the relatively high critical temperature, $T_c\sim 450$ K, for thin ferromagnetic films makes it easier to achieve a small value of the reduced temperature $(T-T_c)/T_c$.

This paper reports the measurements of both components of the complex ac magnetic susceptibility of a number of 2 monolayer (ML) Fe/W(110) films, using the magneto-optic Kerr effect. An unbiased statistical analysis gives the values

of the static critical exponent, $\gamma=1.76\pm 0.06$ and the dynamic critical exponent, $z=2.09\pm 0.06$, (both 95% confidence limits) in agreement with the theory for the 2D Ising model.

II. THEORY

Critical slowing down occurs in systems that are undergoing a second-order phase transition. Fluctuations in the order parameter (which for a ferromagnet is the average magnetization m) at temperatures close to T_c give rise to excitations denoted as δm . For small deviations, the relaxation of the order parameter at temperature T will follow an exponential law given by²⁵

$$\delta m(t) \propto \exp\left[\frac{-t}{\tau(T)}\right], \quad (1)$$

where t is time and τ is the relaxation time. τ is dependent upon the correlation length ξ of the fluctuations in the system. As such, it will diverge at T_c according to a power-law equation given by²⁶

$$\tau(T) = \tau_o \left[\frac{\xi(T)}{\xi_o} \right]^z = \tau_o (\epsilon^{-\nu})^z, \quad (2)$$

where ν is the critical exponent associated with the diverging correlation length ($\nu=1.0$ in the 2D Ising universality class²), τ_o and ξ_o are amplitudes, and ϵ is the reduced temperature given by $[(T-T_c)/T_c]$ above T_c .^{39,40}

The intrinsic magnetic susceptibility of a ferromagnetic system follows a power-law relationship given by

$$\chi_{\text{int}}(T) = \chi_o \epsilon^{-\gamma}, \quad (3)$$

where χ_o is the critical amplitude and γ is the critical exponent of the static susceptibility. This formulation is for the ideal case and does not include experimental complications such as finite-size or dynamical effects, which must be accounted for in an ac-susceptibility measurements. In the presence of a small applied oscillatory magnetic field at frequency ω , the dynamic complex susceptibility in the relaxation approximation becomes

$$\chi_{\text{dyn}}(T) = \frac{1 - i\omega\tau(T)}{1 + \omega^2\tau^2(T)} \chi_{\text{int}}(T). \quad (4)$$

This expression is more complicated if the demagnetization factor of the system is significant. For the 2 ML Fe/W(110) system used in this paper, the extreme aspect ratio of the film, combined with the fact that the magnetic moment is strongly oriented in the plane of the film, should give a demagnetization factor small enough that it can be ignored. This was found to be the case in a previous study¹⁵ of the static exponent γ . With a measurement of the complex ac susceptibility, the value of τ can be derived from the ratio of the imaginary to the real component of the susceptibility²⁷ as follows:

$$\frac{\text{Im}[\chi(T)]}{\omega \text{Re}[\chi(T)]} = \tau(T). \quad (5)$$

This method gives an average value of the relaxation time over the whole of the system.²⁸ It is assumed that this distri-

bution is narrow for a good quality film, so the average value will be sufficient for the measurement.

Experimental limitations prevent the power law divergences in Eqs. (3) and (2) from being observed in experimental data at temperatures right up to T_c . As a sample is cooled towards T_c from above the phase transition, the correlation length will saturate at some value that is dependent on a length scale, such as a sample or grain size, and the measured susceptibility will no longer exhibit power-law scaling. Similarly, the dynamical factor and frequency dependence in Eq. (4) may limit the range of power-law scaling.

III. EXPERIMENT

The measurements of the ac magnetic susceptibility are made from iron bilayers that are grown upon a bcc tungsten single crystal that had been cut and polished to expose the (110) face to within 0.2° . Scanning tunneling microscopy of the substrate performed *ex situ* reveals long terraces of width 500 ± 50 lattice spacings. The films are grown and studied in a UHV system with a base pressure on the order of 10^{-11} torr. They are manufactured using molecular beam epitaxy from a 99.995% pure iron wire source. The thermodynamic stability of an Fe monolayer on W(110) (Refs. 29 and 30) ensures that there is very little mixing at the interface of the film and substrate. It also provides a method to calibrate the iron evaporator and film thickness. Since the first monolayer is very stable when annealed and the second monolayer forms islands when heated above 700 K, it is easy to identify the completion of the first monolayer by a dramatic change in the magnitude of the Auger electron spectroscopy (AES) signal of the W substrate as a function of deposition time.^{30,31} This calibration gives reproducible film thicknesses within ± 0.1 ML.

In growing the samples, the substrate is kept at room temperature during deposition. Upon completion of the first monolayer, the film is annealed to 500 K to ensure proper wetting of the surface. The remaining iron is grown at room temperature and is not annealed afterwards, to avoid islanding of the second layer. The growth and structural properties of Fe/W(110) have been well studied in the past,^{29,32,33} and it forms an epitaxial and pseudomorphic film for at least 2 ML. A (10×10) surface reconstruction begins to develop in the thickness range of 3 to 4 ML. Both AES and low-energy electron diffraction (LEED) techniques are used at each step of the growth process to ensure that the films used in this study conform to those in the previously published studies. According to previous scanning tunneling microscopy studies,^{34,35} these growth procedures should produce films with very nearly complete second layers and a small amount of Fe in the third monolayer.

The magnetic properties are measured using the surface magneto-optic Kerr effect (SMOKE) with a focussed HeNe laser with a diameter of 0.7 mm. The susceptibility is measured using a standard lock-in technique³⁶ which simultaneously determines the real (in-phase) and imaginary (out-of-phase) components. The temperature is measured using a W/W Re thermocouple inserted into the tungsten substrate,

and the rate of temperature increase and decrease is on the order of 0.2 K/minute, which is small enough to remove thermal variations across the film. Heating is accomplished by radiative emission from a small tungsten wire filament located beneath the substrate. The current through the filament is 60 Hz line ac; the effect of any resulting field will be removed by the lock-in detection. Since susceptibilities measured in heating and cooling with different filament currents give indistinguishable results, the magnetic field created by the heating filament is judged to be negligible compared to the applied ac field.

The size of the sinusoidal magnetic field used in susceptibility measurements is an important parameter, and one that requires careful consideration. For this work, a small magnetic field is applied from a set of Helmholtz coils on the sample holder. The size of the field had previously been calibrated at the substrate surface using a Hall probe. The applied magnetic field should be infinitesimally small, which is an experimental impossibility. For practical purposes, if the field is too large, the finite field will saturate $\chi_{\text{dyn}}(T)$ at a higher temperature than does the correlation length, and critical scaling will not be observed. On the other hand, if the field is too small, the signal-to-noise ratio of $\text{Im}[\chi(T)]$ will be too small to allow meaningful analysis for $\tau(T)$. For these samples, a previously published study¹⁵ investigated the effect field amplitude has on the maximum value and the full width at half maximum (FWHM) of the susceptibility peak. It was shown that the susceptibility data are unchanged when measured in an ac magnetic field with an amplitude that is less than 1.0 Oe. For fields greater than 1 Oe, the susceptibility maximum was decreased and the FWHM was increased, clearly affecting the data. Since the data do not change for applied fields less than 1 Oe, some other factor stops the divergence of the susceptibility. The data and analysis presented in the Sec. IV show that this is in fact a dynamical effect. A field of 0.7 Oe was used to maximize the signal-to-noise ratio.

It was not clear *a priori* that this field was small enough to allow the asymptotic critical region to be observed. However, since previous results¹⁵ and the analysis that follows shows that this choice allows the robust extraction of the 2D Ising exponent γ from χ_{dyn} , it is clear *a posteriori* that the field is small enough.

IV. DATA ANALYSIS AND RESULTS

In analyzing any data for critical exponents, the first essential step is to properly determine T_c . This must be done using the susceptibility data. Otherwise, systematic errors will arise from gradual changes in T_c due to residual gas contamination, annealing of the film, and other causes. Since there is no qualitative universal marker for T_c in the shape of the susceptibility curve or the magnetization curve, it is necessary to determine it by fitting. Even though the eventual aim is to find the dynamic critical exponent, the analysis begins by finding the static critical exponent from the real susceptibility, because the relatively large signal permits a statistically significant analysis for T_c . An additional benefit of this approach is the determination of γ , which will ensure

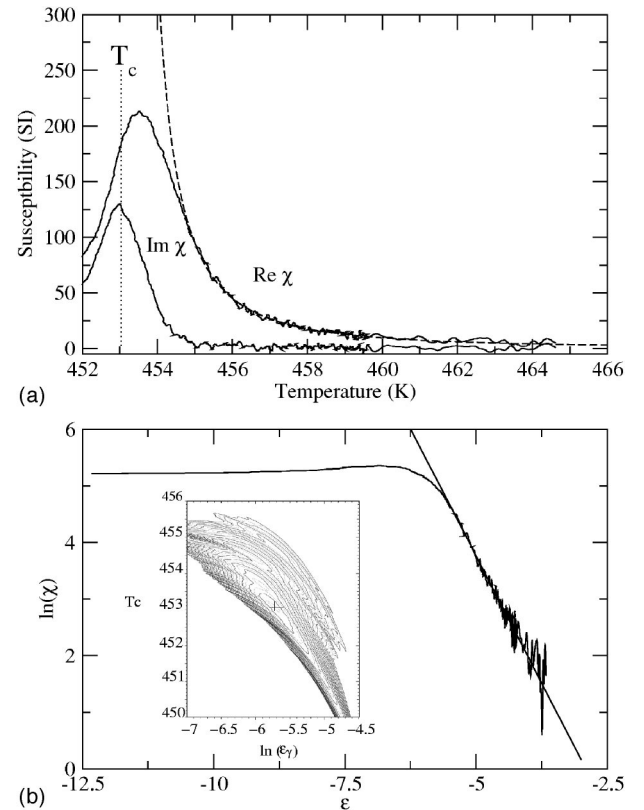


FIG. 1. (a) The real and imaginary components of the magnetic susceptibility measured from a 2 ML Fe/W(110) film. The dashed line shows the power-law fit for the real part used to extract the value for γ and T_c . The dotted line shows the position of $T_c = 453.03$ K. (b) The real susceptibility in double-log space with the fitted line. The inset figure shows a contour plot of the variance of the fit as a function of T_c and the cutoff value of $\ln(\epsilon)$. The minimum (marked by the cross) shows the best fit parameters, and the fit using those parameters is what is shown by the solid line in (b). The solid contours are separated by the variance levels of 2×10^{-4} .

that the film behaves according to the 2D Ising universality class. Since the real and imaginary components of $\chi_{\text{dyn}}(T)$ are measured simultaneously, the same value of T_c can be used in the subsequent analysis for z .

Figure 1(a) shows a typical measurement of the complex ac susceptibility for a 2.0 ± 0.1 ML Fe/W(110) film measured in an applied field of frequency 400 Hz. An objective statistical fitting method (related in greater detail elsewhere¹⁵ and similar to that performed by Arnold and Pappas³⁷) simultaneously fits for the four parameters necessary for an objective analysis. These are the critical temperature T_c , the critical amplitude χ_0 , the critical exponent γ , and the value of the reduced temperature ϵ_γ , where power-law scaling ends near T_c . A weighted linear least-squares fit for χ_0 and γ is performed in double-log space on the susceptibility data range between the maximum temperature measured ϵ_{max} and the cutoff ϵ_γ , using the assumed values of T_c and ϵ_γ . The variance (i.e., reduced statistical χ^2) of the fit as a function of the values of T_c and ϵ_γ is shown in the contour plot inset in Fig. 1(b). The minimum of the variance gives the best values of T_c and ϵ_γ . The best fit is shown in Figs. 1(a) and 1(b). The fitted values of the power law for this data set are γ

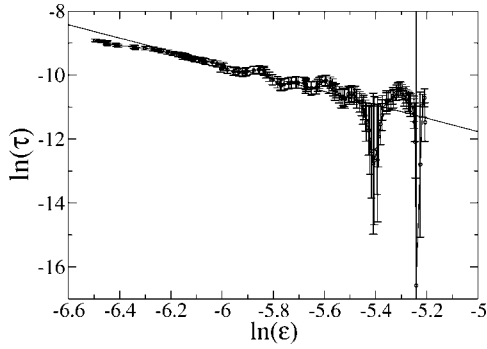


FIG. 2. A double-logarithmic graph of τ plotted against the reduced temperature ϵ . A linear fit is shown over a small-temperature range between the $\ln(\epsilon)$ values of -6.51 and -5.26 . The apparent oscillations in the data are artifacts of the low-frequency noise in the data that is magnified on this double-logarithmic scale.

$=1.80 \pm 0.06$, $\chi_o = 5.53 \pm 0.5 \times 10^{-3}$ (SI units), $T_c = 453.03 \pm 0.02$ K, and $\ln(\epsilon_\gamma) = -5.71$ (approximately 1.5 K above T_c). The error in T_c is found from the change in this parameter required to increase the statistical χ^2 by unity.^{15,38} The value for γ places it within an error of $\frac{7}{4}$, the accepted value for the 2D Ising class. T_c was found to be slightly below the peak in the real susceptibility, in agreement with previous susceptibility measurements on Fe/W(110) films.^{12,15}

Continuing to the next step of the analysis for the relaxation time, the ratio of the complex susceptibility is taken as in Eq. (5). The result is plotted as a function of reduced temperature on a double-log graph to search for a linear segment that shows power-law scaling. Because the real and imaginary $\chi(T)$ are measured simultaneously, the value of the Curie temperature is precisely the same value as determined by the fit for γ . Figure 2 shows that for values of τ between $\ln(\epsilon) = -5.26$ and the cutoff $\ln(\epsilon_z) = -6.51$, there exists a significant linear segment composed of 137 data points. A weighted least-squares fit finds a critical exponent product $z\nu = 2.09 \pm 0.03$ with an amplitude $\tau_o = 2.6 \pm 0.6 \times 10^{-10}$ s. The order of magnitude of the amplitude (inverse GHz) is consistent with the value of τ_o expected from the ferromagnetic resonance (FMR) frequencies. The reduced χ^2 of the fit is 2.69.

Among a number of susceptibility measurements made from two different 2 ML Fe films, two from each film have a large enough number of data points in the range between ϵ_γ and ϵ_z to allow a meaningful analysis for $z\nu$. The individual fitting results are listed in Table I. The resulting average value for γ for these measurements is 1.76 ± 0.06 (95% confidence), in agreement with the 2D Ising value of $\frac{7}{4}$. The average for $z\nu$ is 2.09 ± 0.06 (95% confidence). Since it is well known that the 2D Ising value of ν is 1.0, the product of $z\nu$ is in fact the value for z itself. This measurement of z for a 2D Ising system confirms the current theoretical consensus value within error and conforms to the bound $z \geq 2$.

The internal consistency of the analyses for the static and dynamic critical exponents is illustrated in Fig. 3, which compares the fits to $\ln \chi_{\text{dyn}}$ and $\ln \tau$. On a qualitative level, the fact that the values of ϵ_γ and ϵ_z are different and that the

TABLE I. The fitted values for dynamic scaling from four separate measurements of the complex susceptibility. The statistical errors are 1σ .

Film	ω	γ	$z\nu$	τ_o (s)	ξ_{sat} (ξ_o)
1	$2\pi(400)$	$1.80 \pm .06$	$2.09 \pm .03$	$2.6 \pm 0.6 \times 10^{-10}$	730
1	$2\pi(400)$	$1.67 \pm .10$	$2.01 \pm .07$	$4.0 \pm 0.3 \times 10^{-10}$	720
2	$2\pi(150)$	$1.75 \pm .02$	$2.13 \pm .04$	$1.7 \pm 0.3 \times 10^{-9}$	425
2	$2\pi(150)$	$1.81 \pm .06$	$2.04 \pm .06$	$2.1 \pm 0.5 \times 10^{-9}$	475
average		$1.76 \pm .02$	$2.09 \pm .02$		

ranges of reduced temperature showing power-law scaling in the two curves are different proves that $\ln \chi_{\text{dyn}}$ and $\ln \tau$ are independent measurements which show power-law scaling independently. Furthermore, it is clear that different mechanisms cause the two measurements to saturate close to T_c . A quantitative calculation shows that the susceptibility stops growing like a power law at $\epsilon = \epsilon_\gamma$ because of the dynamical factor in Eq. (4). Using the fitted values of τ_o and $z\nu$ from Fig. 2, the dynamical factor $(\omega\tau)^2 = 0.01$ at ϵ_γ . This is consistent with simple numerical modeling, which shows that departures from linearity on a log-log plot are clearly evident to the eye when $(\omega\tau)^2 \approx 0.05$ in Eq. (4). The finding that dynamical effects determine ϵ_γ is further confirmation that, in these measurements, the static scaling is not affected in an important way by the demagnetization factor nor by the use of too large an ac field.¹⁵

In contrast, the power-law behavior of τ continues closer to T_c , because the dynamical factor cancels out in Eq. (5). Finally, at ϵ_z , τ saturates due to some combination of finite-size and finite-field effects. The following simple analysis allows an estimate to be made for the limiting correlation length, ξ_{sat} , by assuming that it is entirely responsible for the saturation of τ ,

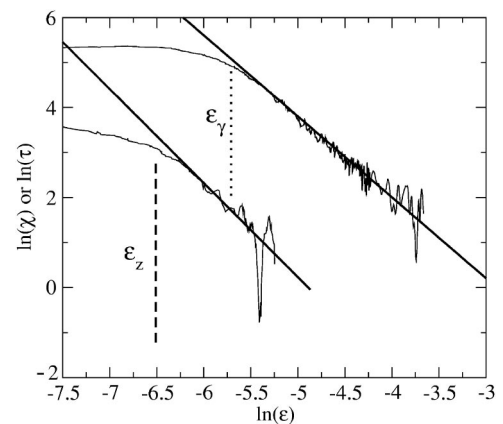


FIG. 3. The power-law scaling in the real susceptibility χ and the relaxation time τ are compared by shifting the data for $\ln(\tau)$ up on a double-logarithmic plot. The cutoff ϵ_z for the linear behavior in $\ln(\tau)$ (lower curve) lies significantly closer to T_c than the cutoff ϵ_γ for the real susceptibility (upper curve).

$$\xi = \begin{cases} \xi_0 \epsilon^{-\nu}, & \epsilon > \epsilon_c \\ \xi_{sat}, & \epsilon \ll \epsilon_c \end{cases} \quad (6)$$

An ansatz to interpolate between these two extremes is

$$\xi = \frac{[\xi_{sat}][(\xi_0 \epsilon^{-\nu})]}{[(\xi_{sat})^\kappa + (\xi_0 \epsilon^{-\nu})^\kappa]^{1/\kappa}}, \quad (7)$$

where κ is a nonuniversal mixing factor that sets the range of the reduced temperature over which ξ goes from power-law behavior to its saturated value. The size of κ is related to the distribution of length scales that act to saturate ξ . Eq. (7) is then substituted into Eq. (2) in order to fit the τ data all the way to T_c . Using the previously fitted values of z and τ_0 , the data fit quite well with $\kappa=2.7$ and $\xi_{sat}/\xi_0=730$, as shown in Fig. 4. Assuming a value of ξ_0 of a single-lattice spacing ($\approx 3 \text{ \AA}$), the value for ξ_{sat} for the data in Fig. 1 is about $.22 \mu\text{m}$. The fitted values for ξ_{sat} for each experiment are collected in Table I. According to a scanning tunneling microscope (STM) survey of the substrate surface, the average step terrace width is 500 ± 50 lattice spacings. The similarity of these length scales suggests that the correlation length is limited by the atomic steps of the surface.

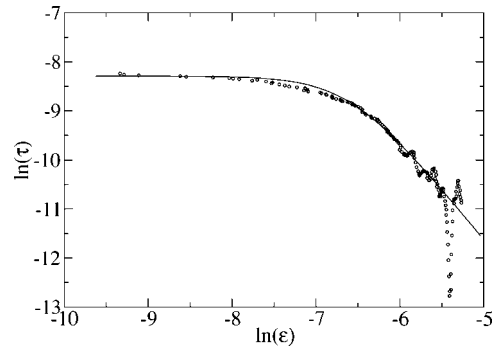


FIG. 4. A double-logarithmic plot of the relaxation time (τ) as a function of the reduced temperature. The solid line shows the fit for ξ_{sat} using a simple model which includes both power-law scaling and saturation regimes.

ACKNOWLEDGMENTS

The authors wish to thank Martin Grant of McGill University and Malcolm Collins of McMaster University for useful discussions. The authors wish to acknowledge the many technical contributions made by Marek Kiela. This work was supported by the Natural Sciences and Engineering Research Council of Canada.

*Electronic address: Michael.Dunlavy@dal.ca

¹P. C. Hohenberg and B. I. Halperin, Rev. Mod. Phys. **49**, 435 (1977).

²M. Collins, *Magnetic Critical Scattering* (Oxford University Press, New York, 1989).

³R. Coldea, R. Cowley, T. Perring, D. McMorrow, and B. Roessli, Phys. Rev. B **57**, 5281 (1998).

⁴S.-H. Tsai and D. Landau, Phys. Rev. B **67**, 104411 (2003).

⁵F. Livet, F. Bley, J.-P. Simon, R. Caudron, J. Mainville, M. Sutton, and D. Lebolloch, Phys. Rev. B **66**, 134108 (2002).

⁶V. Aji and N. Goldenfeld, Phys. Rev. Lett. **87**, 197003 (2001).

⁷R. J. Christianson, R. L. Leheny, R. J. Birgeneau, and R. W. Erwin, Phys. Rev. B **63**, 140401(R) (2001).

⁸P. Archambault, S. Bramwell, and P. Holdsworth, J. Phys. A **30**, 8363 (1997).

⁹N. D. Mermin and H. Wagner, Phys. Rev. Lett. **17**, 1133 (1966).

¹⁰M. Bander and D. L. Mills, Phys. Rev. B **38**, 12 015 (1988).

¹¹H.-J. Elmers, Int. J. Mod. Phys. B **9**, 3115 (1995).

¹²H. J. Elmers, J. Hauschild, and U. Gradmann, Phys. Rev. B **54**, 15 224 (1996).

¹³Y. Li and K. Baberschke, Phys. Rev. Lett. **68**, 1208 (1992).

¹⁴C. H. Back, C. Würsch, A. Vaterlaus, U. Ramsperger, U. Maler, and D. Pescia, Nature (London) **378**, 597 (1995).

¹⁵M. J. Dunlavy and D. Venus, Phys. Rev. B **69**, 094411 (2004).

¹⁶M. D. Lacasse, J. Vinals, and M. Grant, Phys. Rev. B **47**, 5646 (1993).

¹⁷M. Nightingale and H. Blöte, Phys. Rev. Lett. **76**, 4548 (1996).

¹⁸S. Wansleben and D. P. Landau, Phys. Rev. B **43**, 6006 (1991).

¹⁹K. Chen and D. P. Landau, Phys. Rev. B **49**, 3266 (1994).

²⁰R. Bausch, V. Dohm, H. Janssen, and R. Zia, Phys. Rev. Lett. **47**,

1837 (1981).

²¹M. Grant, Phys. Rev. Lett. **62**, 1065 (1989).

²²J. Slivka, H. Keller, W. Kundig, and B.M. Wanklyn, Phys. Rev. B **30**, 3649 (1984).

²³H. Keller and I. M. Savic, Phys. Rev. B **28**, 2638 (1983).

²⁴M. T. Hutchings, H. Ikeda, and E. Janke, Phys. Rev. Lett. **49**, 386 (1982).

²⁵M. Mori and Y. Tsuda, Phys. Rev. B **37**, 5444 (1988).

²⁶N. Goldenfeld, *Lectures on Phase Transitions and the Renormalization Group* (Addison-Wesley Publishing Co., Reading, MA, 1992).

²⁷A. T. Ogielski, Phys. Rev. B **32**, 7384 (1985).

²⁸N. Bontemps, J. Rajchenbach, R. V. Chamberlin, and R. Orbach, Phys. Rev. B **30**, 6514 (1984).

²⁹U. Gradmann, M. Przybylski, H. J. Elmers, and G. Liu, Appl. Phys. A: Solids Surf. **49**, 563 (1989).

³⁰P. Berlowitz, J. He, and D. Goodman, Surf. Sci. **231**, 315 (1990).

³¹D. Venus, Phys. in Canada **55**, 267 (1999).

³²J. Kolaczkiwicz and E. Bauer, Surf. Sci. **450**, 106 (2000).

³³U. Gradmann and G. Waller, Surf. Sci. **116**, 539 (1982).

³⁴H. J. Elmers, J. Hauschild, H. Fritzsche, G. Liu, U. Gradmann, and U. Kohler, Phys. Rev. Lett. **75**, 2031 (1995).

³⁵H. Bethge, D. Heuer, C. Jensen, K. Reshöft, and U. Köler, Surf. Sci. **331–333**, 878 (1995).

³⁶C. S. Arnold, M. J. Dunlavy, and D. Venus, Rev. Sci. Instrum. **68**, 4212 (1997).

³⁷C. S. Arnold and D. P. Pappas, Phys. Rev. Lett. **85**, 5202 (2000).

³⁸P. Bevington and D. Robinson, *Data Reduction and Error Analysis for the Physical Sciences* (McGraw-Hill Inc., New York, 1992).

³⁹An alternate formulation of dissipation uses the Landau-Lifshitz (Ref. 40) damping parameter $\lambda: \partial m / \partial t = -\lambda H_{eff} = -\lambda[(m / \chi_{eff}) - H]$. Analysis of λ has the advantage of removing from the slowing down exponent that portion of the temperature dependence which is due to the divergence of the static susceptibility.

The relationship between the two formulations is $\tau = \chi_{eff} / \lambda$. We use Eq. (1) to allow comparison to the majority of theoretical work.

⁴⁰L. Landau and E. Lifshitz, Phys. Z. Sowjetunion **8**, 153 (1935).